MOLECULAR AND CELLULAR BIOLOGY, Nov. 1993, p. 6690–6701
0270-7306/93/116690-12$02.00/0

Vol. 13, No. 11

Identification of a Killer Cell-Specific Regulatory Element of the Mouse Perforin Gene: an Ets-Binding Site-Homologous Motif That Interacts with Ets-Related Proteins

HIROTAKA KOIZUMI,[1]† M. FATIMA HORTA,[1] BYUNG-S. YOUN,[2] KOK-CHIN FU,[1] BYOUNG S. KWON,[2] JOHN DING-E YOUNG,[1] AND CHAU-CHING LIU[1]*

Laboratory of Molecular Immunology and Cell Biology, The Rockefeller University, 1230 York Avenue, New York, New York 10021,[1] and Department of Microbiology and Immunology, Indiana University School of Medicine, Indianapolis, Indiana 46202[2]

Received 11 March 1993/Returned for modification 29 April 1993/Accepted 9 August 1993

The gene encoding the cytolytic protein perforin is selectively expressed by activated killer lymphocytes. To understand the mechanisms underlying the cell-type-specific expression of this gene, we have characterized the regulatory functions and the DNA-protein interactions of the 5′-flanking region of the mouse perforin gene (*Pfp*). A region extending from residues +62 through −141, which possesses the essential promoter activity, and regions further upstream, which are able to either enhance or suppress gene expression, were identified. The region between residues −411 and −566 was chosen for further characterization, since it contains an enhancer-like activity. We have identified a 32-mer sequence (residues −491 to −522) which appeared to be capable of enhancing gene expression in a killer cell-specific manner. Within this segment, a 9-mer motif (5′-ACAGGAAGT-3′, residues −505 to −497; designated NF-P motif), which is highly homologous to the Ets proto-oncoprotein-binding site, was found to interact with two proteins, NF-P1 and NF-P2. NF-P2 appears to be induced by reagents known to up-regulate the perforin message level and is present exclusively in killer cells. Electrophoretic mobility shift assay and UV cross-linking experiments revealed that NF-P1 and NF-P2 may possess common DNA-binding subunits. However, the larger native molecular mass of NF-P1 suggests that NF-P1 contains an additional non-DNA-binding subunit(s). In view of the homology between the NF-P motif and other Ets proto-oncoprotein-binding sites, it is postulated that NF-P1 and NF-P2 belong to the Ets protein family. Results obtained from the binding competition assay, nevertheless, suggest that NF-P1 and NF-P2 are related to but distinct from Ets proteins, e.g., Ets-1, Ets-2, and NF-AT/Elf-1, known to be expressed in T cells.

Perforin, the pore-forming protein (PFP), is a cytolytic protein specifically expressed in killer lymphocytes, including cytotoxic T lymphocytes (CTL), natural killer cells, lymphokine-activated killer (LAK) cells, and γ/δ T cells. Together with other effector molecules, PFP is thought to play a crucial role in lymphocyte-mediated cytotoxicity by forming transmembrane pores that lead to target cell lysis (18, 32, 42, 48).

We and others have previously shown that perforin message level can be up-regulated by a variety of T-cell activators such as interleukin-2 (IL-2), lectins, and phorbol ester and is partially down-regulated by the immunosuppressive drug cyclosporin A (15, 23, 24). Results obtained from these studies, however, provided no clues to the mechanisms that control the cell-type-specific expression of the perforin gene (*Pfp*). Recently, the genomic organizations of mouse and human *Pfp* have been defined (21, 41, 47). Their 5′-flanking sequences, being homologous to each other, share also some homology with known *cis*-acting elements (21, 47). In the case of mouse *Pfp*, these include TATA box- and GC box-related promoter sequences; cyclic AMP-, phorbol ester-, and gamma interferon-responsive site-like elements; and NF-κB binding site-like elements (summarized in Fig. 1A) (47). Although it appears that these potential elements and their cognate *trans*-acting factors are involved in regulating the transcription of *Pfp*, virtually no information is available concerning the regulatory functions and the DNA-protein interactions of the *Pfp* 5′-flanking region.

The tissue- and cell-specific manner of gene expression has been shown to rely primarily on the combined actions of various transcription factors. These transcription factors may interact with their cognate regulatory sequences (promoters, enhancers, or silencers) of the gene to be transcribed (27, 29). The presence of multiple regulatory elements allows specific transcription factors to initiate efficient transcription in a coordinated manner within a cell at different times during its growth, differentiation, or activation. Mechanisms that control the expression of lymphocyte-specific genes have recently been elucidated, mainly through the studies on T-cell receptor and immunoglobulin genes. It has been shown that T- or B-cell-specific nuclear factors, such as TCF-1/LEF-1, GATA-3, and OTF-2/Oct-2, are involved in restricting the expression of T-cell receptor or immunoglobulin genes to lymphocytes by interacting with their cognate *cis*-acting elements (20, 35). On the basis of the premise that killer lymphocytes should also contain their particular transcription factors to regulate *Pfp* expression, we have attempted to localize the functional DNA sequences which control *Pfp* expression in killer cells.

In this paper, we report the identification of the promoter region and several additional upstream regulatory sequences of *Pfp*. Among these sequences, a 32-bp segment (residues −522 to −491) appears to be capable of driving gene expres-

* Corresponding author.
† Present address: Department of Pathology II, St. Marianna University School of Medicine, 2-16-1 Sugao, Miyamae-Ku, Kawasaki 216, Japan.

sion in a killer cell-specific fashion. This segment contains a 9-mer motif located between residues −505 and −497 which is homologous to the Ets proto-oncoprotein-binding site (EBS). We present results suggesting that this 9-mer motif probably plays a role in controlling *Pfp* expression in killer cells.

MATERIALS AND METHODS

Cells. Murine cell lines P815 (mastocytoma), YAC-1 (T-cell leukemia), and EL-4 (thymoma) were maintained in α-modified minimal essential medium supplemented with 5% fetal calf serum (Hyclone Laboratories, Logan, Utah) and antibiotics. IL-2-dependent CTL lines CTLL-R8 and CTLL-2 were further supplemented with 10% conditioned medium [the culture supernatant of rat splenocytes stimulated for 48 h with 10 μg of concanavalin A (ConA; Sigma Chemical Co., St. Louis, Mo.) per ml and 20 ng of phorbol myristyl acetate (PMA) (Sigma) per ml] (15, 23). The resting CTLL-R8 cells were prepared by depriving confluent R8 cells of the conditioned medium for 1 week prior to being used in the experiments. In some experiments, EL-4 and resting CTLL-R8 were stimulated for 24 h with 100 U of recombinant human IL-2 (Cetus Corp., Emeryville, Calif.) per ml, ConA and PMA (10 μg and 20 ng, respectively, per ml), or 10% conditioned medium. Murine spleens and livers were obtained from young C57BL/6 mice. Adherent LAK cells were derived from nylon-wool-purified splenic T cells (15, 49).

Plasmid constructs. A panel of plasmid constructs containing sequential deletion of the *Pfp* 5′-flanking sequence fused to a reporter gene, chloramphenicol acetyltransferase (CAT), was prepared. An artificial fragment of *Pfp* 5′-flanking region was generated by polymerase chain reaction (PCR) with a 5′ primer that incorporated a *Sac*I site into the sequence encoding residues −700 through −684 of the mouse *Pfp* and a 3′ primer complementary to residues +45 through +62 plus a *Hin*dIII site. The PCR-amplified fragments were digested with *Sac*I and *Hin*dIII and then cloned into a *Sac*I-*Hin*dIII-digested pSVCAT vector which contains the simian virus 40 early promoter and the CAT gene so that the *Pfp* 5′ sequence would be located upstream to the CAT gene and downstream to the simian virus 40 promoter. To create shorter deletional constructs, the original reporter construct was linearized with *Sac*I and digested with *Bal* 31 nuclease for different lengths of time, and the inserts were released by *Hin*dIII digestion, purified, and polished by *Sac*I linker ligation and then by *Sac*I digestion. The shortened inserts were finally ligated into *Sac*I-*Hin*dIII-digested pSVCAT vector, and the precise 5′ edge of the *Pfp* regulatory sequence in each prepared construct was determined by nucleotide sequencing. Alternatively, the longer insert was cleaved with *Pvu*II enzyme at residues −522 and −141, and the desired fragment was purified, polished, and cloned into the vector. This series of reporter plasmids was designated $pCAT_{000}$ ($_{000}$ indicates the 5′ edge of the *Pfp* sequence incorporated) constructs. To analyze the function of the NF-P motif, two types of constructs were prepared. An oligonucleotide encoding three copies of the *Pvu*II-*Kpn*I fragment sequence (residues −522 through −491) in tandem was synthesized and inserted upstream of the *Pfp* 5′ sequence in $pCAT_{-411}$ (containing *Pfp* 5′ sequence up to residue −411). DNA fragments containing mutation within the NF-P motif were amplified by PCR with the universal 3′ primer and mutated oligonucleotides (M2 and M3 [see below]) as the 5′ primer. These fragments (corresponding to residues −522 through +62 of the *Pfp* sequence) were subcloned into the pSVCAT vector, and mutations of the NF-P motif were verified by sequencing.

DNA transfection. Plasmids twice purified by CsCl banding were transfected into cells by electroporation. Briefly, 5×10^6 cells in 400 μl of phosphate-buffered saline (PBS) were electroporated in the presence of 40 μg of plasmid DNA at 960 μF and 280 V (CTLL-R8) or 300 V (EL-4 and P815), in a 4-mm-diameter electroporation cuvette by using a Bio-Rad Gene Pulser (Richmond, Calif.). After incubation for 10 min on ice, electroporated cells were transferred to 150-mm-diameter petri dishes containing prewarmed media and incubated for 48 h.

CAT assay. CAT activity in the transfected cells was tested by using a CAT enzyme assay kit (Promega Co., Madison, Wis.). Cell extracts for CAT assay were prepared by freezing and thawing cells three times in 150 μl of 0.25 M Tris-HCl, pH 8.0. The extracts were heated at 60°C for 10 min to inactivate endogenous acetylase and spun for 10 min to remove particulate debris. The level of CAT activity was normalized to the amount of CAT plasmid DNA introduced by transfection, as determined by DNA dot blot analysis (1). Briefly, 10 μl of cell extract was sequentially incubated at 37°C for 30 min (each) with RNase A (100 μg/ml) and then with proteinase K (100 μg/ml). After incubation, 2 volumes of 20× SSC (1× SSC is 0.15 M NaCl plus 0.015 M sodium citrate) was added, and the DNA was denatured in 0.25 N NaOH for 10 min at room temperature. Samples were serially diluted on prechilled 0.125 N NaOH–0.125× SSC and dotted onto GeneScreen Plus membranes (New England Nuclear, Boston, Mass.). Membranes were prehybridized for 30 min and hybridized to ^{32}P-labeled pCAT DNA. After being washed, the membranes were subjected to autoradiography. The volumes of the cell extracts used in CAT assay were normalized to the relative amount of transfected CAT DNA, determined by the intensities of the hybridization signals. The reaction mixture containing the normalized volume of cell extract, 25 μg of *n*-butyryl coenzyme A, and 0.05 μCi of [^{14}C]chloramphenicol (New England Nuclear) supplemented with 0.25 M Tris-HCl, pH 8.0, to a final volume of 125 μl. The reaction was carried out at 37°C overnight, with an additional 25 μg of *n*-butyryl coenzyme A added at 2 to 4 h after the initiation of the reaction. The amount of acetylated chloramphenicol produced was determined either by liquid scintillation counting or by thin-layer chromatography.

Electrophoretic mobility shift assay (EMSA). Cell nuclear extracts (NEs) were prepared as previously described (8, 11). Briefly, cells were washed three times with PBS, resuspended in 3 pelleted cell volumes of buffer A (10 mM *N*-2-hydroxyethylpiperazine-*N*′-2-ethanesulfonic acid [HEPES; pH 7.9], 1.5 mM $MgCl_2$, 10 mM KCl, 0.2 mM phenylmethylsulfonyl fluoride [PMSF], 0.5 mM dithiothreitol [DTT]), incubated on ice for 10 min, homogenized with a Dounce homogenizer (10 strokes, type B pestle), and centrifuged at 1,000 × *g* to sediment the nuclei. The nucleus pellet was resuspended in a 0.5 packed-nuclei volume of buffer B (20 mM HEPES [pH 7.9], 1.5 mM $MgCl_2$, 20 mM KCl, 0.2 mM EDTA, 0.5 mM PMSF, 0.5 mM DTT, 25% [vol/vol] glycerol). A 0.5 packed-nuclei volume of buffer C (20 mM HEPES [pH 7.9], 1.5 mM $MgCl_2$, 1.2 M KCl, 0.2 mM EDTA, 0.5 mM PMSF, 0.5 mM DTT, 25% glycerol) was subsequently added drop by drop with constant agitation. The nuclei were extracted at 4°C for 30 min and centrifuged at 10,000 × *g* for 30 min. The supernatant collected was dialyzed against 50 volumes of buffer D (20 mM HEPES [pH

7.9], 100 mM KCl, 0.2 mM EDTA, 0.2 mM PMSF, 0.5 mM DTT) for 1 h and clarified by centrifugation at 10,000 × *g* for 20 min. The NEs thus prepared were stored at −70°C until use. NE of HeLa cells was obtained from Stratagene (La Jolla, Calif.). Protein concentrations were determined by the Bradford method (6) with a Bio-Rad assay kit.

An *Nco*I-*Kpn*I fragment of the 5′ region of *Pfp* (residues −609 through −491) was labeled with [α-^{32}P]dCTP by using Klenow fragment. Double-stranded oligonucleotides were labeled with [γ-^{32}P]ATP and T4 polynucleotide kinase and purified by polyacrylamide gel electrophoresis (PAGE). A typical binding reaction mixture (25-μl final volume) consisted of 5 μg of NE, 2 × 10^4 cpm of end-labeled probe (0.2 to 0.5 ng), 2.5 μg of poly(dI-dC) (Pharmacia LKB, Piscataway, N.J.), 25 mM Tris-HCl (pH 7.9), 6.25 mM $MgCl_2$, 0.5 mM EDTA, 50 mM KCl, 0.5 mM DTT, and 10% glycerol. After incubation for 20 min at 0°C, the resulting DNA-protein complexes were resolved from the free probe by electrophoresis on a 6% native polyacrylamide gel and visualized by autoradiography.

Synthetic oligonucleotides. The coding-strand sequences of synthetic oligonucleotides are shown in Fig. 3C (overlapping oligonucleotides, OL 1 to 3), Fig. 4A (multiple-base mutations, M1 to 4), and Fig. 4B (one-point mutations, OP 1 to 10). Mutations were designed to substitute purines with the nonpairing pyrimidine residues and vice versa. An oligonucleotide containing the Ets-1 binding site was synthesized as a 32-mer (5′-TTCCAGAGGATGTGGCTTCTGCGGGAG AGCTT) derived from the reported sequence (13), and the 30-bp oligonucleotide containing the NF-AT binding site was kindly provided by A. Granelli-Piperno (The Rockefeller University) (12).

UV cross-linking experiment. In situ UV cross-linking of DNA-protein with end-labeled OL 2 was performed by the established procedure (30) with some modifications. After resolution by EMSA, the gels were subjected to autoradiography briefly to locate the DNA-protein complexes. The areas identified were excised, pooled in 35-mm-diameter petri dishes, and irradiated with UV for 1 h. Alternatively, the gels were first subjected to UV irradiation (2,500 mJ) by using a Stratalinker (Stratagene), and the areas containing the DNA-protein complexes were located by autoradiography and excised. The cross-linked DNA-protein complexes were then collected by either electroelution or passive diffusion into the soaking buffer, boiled in sodium dodecyl sulfate (SDS)-containing loading buffer, and resolved by SDS–10 or 6% PAGE. After electrophoresis, the gel was dried under vacuum and subjected to autoradiography. Controls for this type of experiment included SDS-PAGE of the DNA-protein complexes eluted from a nonspecific band on EMSA following UV cross-linking or of the complexes without being cross-linked by UV irradiation prior to SDS-PAGE.

RESULTS

Functional mapping of the mouse *Pfp* promoter and regulatory regions. Although several potential regulatory elements in mouse *Pfp* have been identified by sequence comparison (Fig. 1A), functional relevances of these elements have not yet been established. Recently, several groups, including ours, have attempted to address this issue (22, 40). To locate the promoter region that potentially regulates *Pfp* expression, we have constructed a series of plasmids that contain 5′ sequential deletions of mouse *Pfp* 5′-flanking region fused to the CAT gene. Since reporter

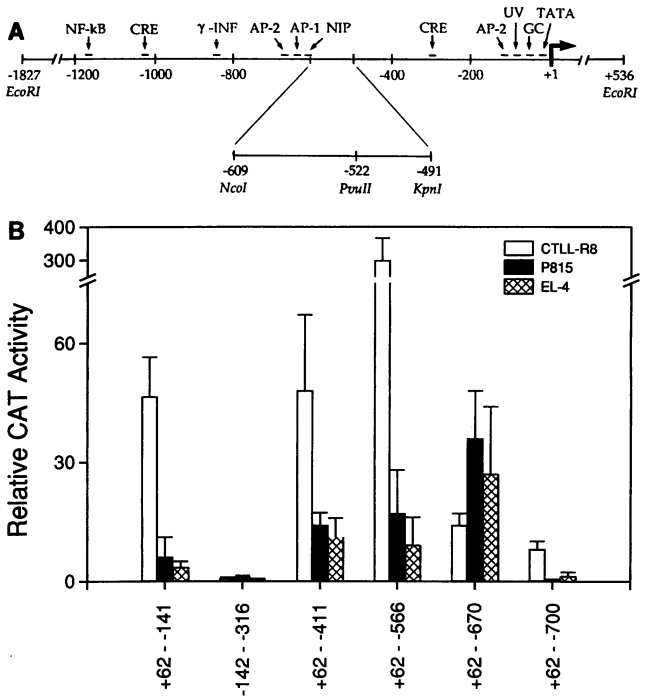

FIG. 1. Sequence comparison and functional analysis of the 5′-flanking region of mouse *Pfp*. (A) Alignment of the potential regulatory elements identified by computer-assisted sequence comparison. (B) CTLL-R8, EL-4, and P815 cells were transiently transfected with the pCAT reporter construct. To adjust for the different transfection efficiencies, volumes of cell extracts containing the same amount of plasmid DNA as determined by dot blot analysis (see Materials and Methods) were used for CAT assays. The CAT activities were determined by liquid scintillation counting and normalized against the activity obtained from cells transfected with the pSVCAT vector, which usually gave no or low counts. The result for each construct was derived from at least three independent experiments.

constructs prepared in a plasmid vector which contains the CAT gene alone drove the expression of the CAT gene only weakly, we generated constructs with similar 5′-flanking sequences cloned into a plasmid vector containing the CAT gene and the early promoter of simian virus 40 in order to potentiate the activity of the *Pfp* sequences. These constructs were transiently expressed in both CTLs and non-CTLs, and the levels of CAT expression were normalized against the expression driven by the simian virus 40-CAT vector. Although the region encompassing nucleotides +62 through −141 (transcription initiation site as +1) was able to drive the expression of CAT in CTLL-R8, EL-4, and P815 cells, a much higher efficiency was observed in CTLL-R8 (47-fold) than in nonkiller cells (4-fold for EL-4 and 6-fold for P815) (Fig. 1B). These results suggest that a basal promoter activity for *Pfp* is present within this region. Incorporation of the sequence between residues −142 through −411 into the construct failed to drive more CAT expression (comparing the results obtained with $pCAT_{+62\ to\ -141}$ and $pCAT_{+62\ to\ -411}$, respectively), suggesting that this region does not contain strong regulatory elements (Fig. 1B). Notably, a construct ($pCAT_{-142\ to\ -316}$) lacking the sequence encompassing residues +62 through −141 lost its ability to drive the CAT expression, indicating again that the essential promoter activity for *Pfp* resides within the 5′-flanking sequence up to residue −141.

Inclusion of sequence extending to residue −566 in the reporter construct enhanced CAT expression profoundly in CTLL-R8 but only slightly in EL-4 and P815 cells (Fig. 1B). Further extension of the *Pfp* 5′-flanking sequence to residue −670 and residue −700, however, reduced the CAT gene expression in all three cell types examined. These results suggest that a killer cell-specific positive regulatory element(s) is present between residue −412 and −566. Therefore, we decided to further characterize this region.

DNA-protein interactions in the *Nco*I-*Kpn*I region (residues −609 through −491) of mouse *Pfp*. Since DNA-binding proteins may represent *trans*-acting factors that affect the transcription of *Pfp*, we first set out to identify proteins that interact with the −566 to −412 sequence. To circumvent the limitation of available restriction sites surrounding this region, we initially used a 119-bp *Nco*I-*Kpn*I fragment (residues −609 through −491) as a probe in EMSA to examine the 5′ end of the region of interest. Comparing the electrophoretic profile of unstimulated CTLL-R8 (Fig. 2A, lane 1) with that of the CTLL-R8 stimulated with conditioned medium, IL-2, or ConA and PMA (lanes 2 to 4, respectively), it was noted that the amount of a DNA-protein complex (designated B1) was reduced, and concomitantly, the amount of another complex (designated B2) was reciprocally induced in the stimulated cells. This phenomenon was also observed for primary killer cells. The electrophoretic profile of adherent LAK cells, which were derived from IL-2-stimulated splenic T lymphocytes (15, 49), showed a strong B2 band and a faint B1 band (lane 6), whereas that of the unstimulated splenic T cells displayed only the B1 band (not shown). Interestingly, the electrophoretic profile of confluent resting CTLL-R8 cells (see Materials and Methods) exhibited an intermediate pattern, with the B1 and B2 bands equally present (lane 5). B1 and B2 bands were also observed in the electrophoretic profile of another CTL line, CTLL-2, maintained in conditioned medium (not shown). A third DNA-protein complex, located below the B2 band and present at variable intensities in different cells, was not further investigated since it was not modulated by the T-cell activators (Fig. 2A).

Another DNA fragment, *Kpn*I-*Hin*PI (residues −490 through −263), was similarly tested in the binding assay to examine the effect of the rest of the targeted region (residues −566 through −412). However, DNA-protein complexes formed by this probe displayed similar electrophoretic patterns in both unstimulated and stimulated CTLL-R8 cells (not shown). These results suggest that the B1-B2 modulation observed with the *Nco*I-*Kpn*I fragment may solely account for the increased transcription of the CAT gene driven by the sequence between residues −412 and −566 in CTLL-R8 (Fig. 1B).

To verify the cell-type specificity of B1 and B2 formation, we have also tested nonlymphoid cells (primary hepatocytes, P815, and HeLa cells [Fig. 2A, lanes 7 and 8, and not shown, respectively]) and nonkiller T lymphocytes (YAC-1 and EL-4 [Fig. 2A, lanes 9 and 10 to 12, respectively]) in EMSA by using the *Nco*I-*Kpn*I probe. B1 was found to be ubiquitously present in all cell types tested. B2, on the other hand, appeared to be killer cell specific, since it was not present in EL-4 cells stimulated with conditioned medium, IL-2, or ConA and PMA (Fig. 2A, lanes 11 to 13, respectively, compared with unstimulated EL-4 cells, lane 10). Furthermore, these stimuli failed to reduce B1 in EL-4. Similar results were observed in a human non-CTL T-cell line, Jurkat, stimulated with phytohemagglutinin and PMA (12) (not shown). Thus, the occurrence of the B1-B2 modulation appeared to be restricted to activated killer cells, suggesting its involvement in regulating the transcription of *Pfp* in a cell-type-specific manner.

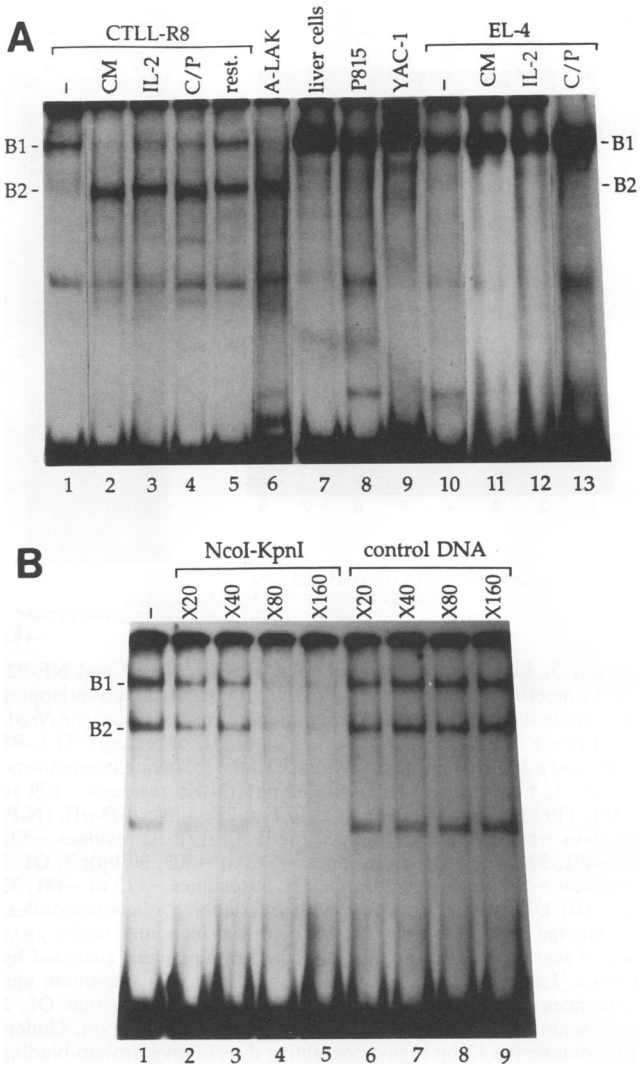

FIG. 2. Binding of nuclear factors to the *Nco*I-*Kpn*I (residues −609 to −491) region. (A) Cell type distribution of B1 and B2. Five micrograms of NE was incubated with an *Nco*I-*Kpn*I probe (0.2 ng, 2×10^4 cpm), and the resulting complexes were analyzed by EMSA. Lanes: 1, unstimulated CTLL-R8; 2, conditioned medium (CM)-stimulated CTLL-R8; 3, IL-2-stimulated CTLL-R8; 4, ConA- and PMA (C/P)-stimulated CTLL-R8; 5, resting (rest.) CTLL-R8; 6, adherent LAK (A-LAK) cells; 7, liver cells; 8, P815; 9, YAC-1; 10, unstimulated EL-4; 11, conditioned medium-stimulated EL-4; 12, IL-2-stimulated EL-4; 13, ConA- and PMA-stimulated EL-4. (B) Sequence specificity of B1 and B2. Lanes: 1, no competitor; 2 to 5, 20-, 40-, 80-, and 160-fold molar excess, respectively, of unlabeled *Nco*I-*Kpn*I fragment (119 bp); 6 to 9, 20-, 40-, 80-, and 160-fold molar excess, respectively, of an unrelated competitor derived from pBluescript SK+ (*Pvu*II-*Kpn*I, 129 bp [Stratagene]). NE of resting CTLL-R8 cells were used in the binding reaction media.

To examine the sequence specificity of B1 and B2 complexes, the *Nco*I-*Kpn*I fragment and a similar-length fragment were used in a binding competition assay. Both complexes were specifically inhibited by the *Nco*I-*Kpn*I fragment (Fig. 2B, lanes 2 to 5) but not by the control

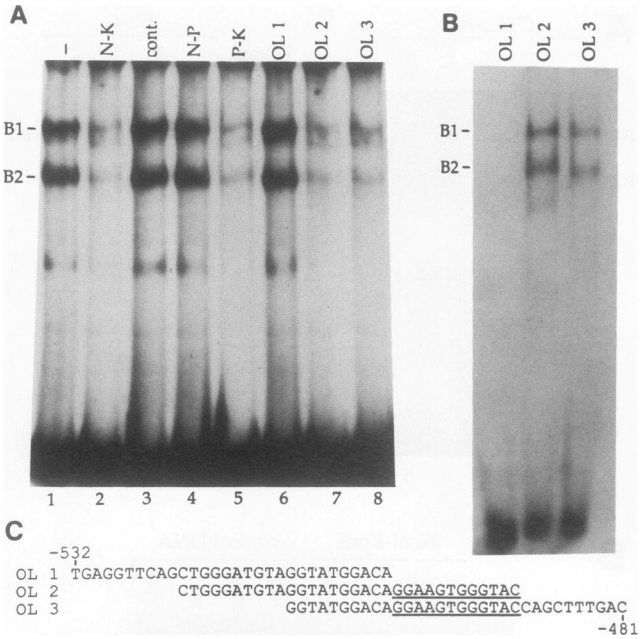

FIG. 3. Localization of the binding site for NF-P1 and NF-P2. (A) Competition of complexes by DNA fragments and overlapping oligonucleotides. The binding reaction mixtures contained the *Nco*I-*Kpn*I probe (0.2 ng, 2×10^4 cpm), 5 μg of NE of resting CTLL-R8 cells, and a 100-fold molar excess each of the following competitors. Lanes: 1, no competitor; 2, *Nco*I-*Kpn*I (N-K; residues −609 to −491, 119 bp); 3, control DNA, as in Fig. 2B; 4, *Nco*I-*Pvu*II, (N-P; residues −609 to −523, 87 bp); 5, *Pvu*II-*Kpn*I (P-K; residues −522 to −491, 32 bp); 6, OL 1 (residues −532 to −503, 30 bp); 7, OL 2 (residues −522 to −491, 32 bp); 8, OL 3 (residues −512 to −481, 32 bp). (B) Direct binding assay with overlapping oligonucleotides. ^{32}P-labeled oligonucleotide (2×10^4 cpm) was incubated with 5 μg of NE of resting CTLL-R8 cells, and the samples were analyzed by EMSA. Lanes 1 to 3, OL 1 to 3, respectively. (C) Alignment and sequences of the overlapping oligonucleotides. Note that OL 2 represents the *Pvu*II-*Kpn*I (residues −522 to −491) region. Underlines denote the 12-bp region containing the putative protein-binding sites (see text).

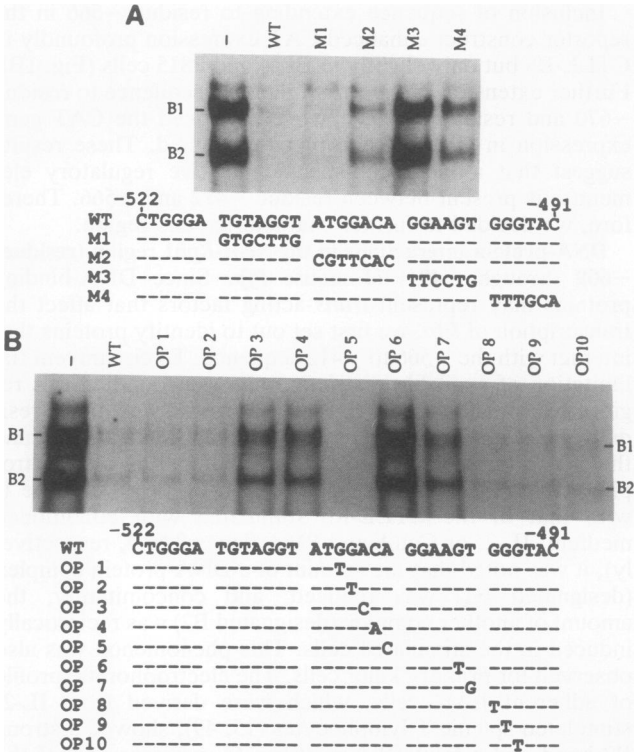

FIG. 4. Identification of the protein-binding sequence. (A) Upper panel: competition assay with multiple-base mutated oligonucleotides (M1 to 4). End-labeled OL 2 was incubated with 5 μg of NE of resting CTLL-R8 cells in the absence of the competitor (−) or in the presence of a 100-fold molar excess of the wild-type OL 2 (WT) or M 1 to 4. Lower panel: nucleotide sequences of M 1 to 4. The sequences are aligned with the wild-type OL 2, and identical bases are denoted by dashes. (B) Upper panel: competition assay with one-point mutated oligonucleotides (OP 1 to 10). The experiment was performed exactly the same as for panel A, except for the use of OP 1 to 10. Lower panel: location of the nucleotide substituted in OP 1 to 10. OP 1 to 5 and OP 8 to 10 contain mutations 5′ and 3′, respectively, to the putative core sequence GGAAGT. OP 6 and 7 are mutants of the core sequence (see text).

fragment, even at the highest concentration tested (lanes 6 to 10). In the following, the nuclear factors that form the ubiquitous B1 and the killer cell-specific B2 will be referred to as NF-P1 and NF-P2, respectively.

Localization of the binding sites for NF-P1 and NF-P2. To localize the binding sites for NF-P1 and NF-P2, the *Nco*I-*Kpn*I fragment (residues −609 through −491) was digested with *Pvu*II to generate two smaller fragments for use in the binding competition assay. The *Pvu*II-*Kpn*I fragment (residues −522 through −491) was able to inhibit both the B1 and the B2 complexes (Fig. 3A, lane 5) as effectively as the intact *Nco*I-*Kpn*I fragment (lane 2), whereas the *Nco*I-*Pvu*II fragment (residues −609 through −523) (lane 4) displayed no such effect at all. These results revealed that the protein-binding sites for both factors reside within the 32-bp *Pvu*II-*Kpn*I fragment. Overlapping oligonucleotides (OL 1 to 3 [Fig. 3C]), of which OL 2 is identical to the *Pvu*II-*Kpn*I region, were then used in the competition assay to define further the sites involved in DNA-protein interaction. Both complexes were specifically inhibited by OL 2 and OL 3 (lanes 7 and 8) but not by OL 1 (lane 6). Direct binding assay also showed that OL 1 could not form B1 and B2 complexes, whereas both OL 2 and OL 3 did (Fig. 3B). In view of the identical behaviors of OL 2 and OL 3 in these experiments, it is concluded that a 12-bp DNA region, where OL 2 overlaps with OL 3 but not with OL 1 (residues −504 through −491 [underlined in Fig. 3C]), contains the binding site(s) for both NF-P1 and NF-P2.

Identical DNA sequence recognized by NF-P1 and NF-P2. Segments of the 32-bp sequence of OL 2 were then mutated to test their effects on complex formation (oligonucleotides M 1 to 4, Fig. 4A). M 3 and M 4, representing mutation in the 12-bp putative binding sequence (Fig. 3C), and M 1 and M2, containing irrelevant mutation in the flanking region, were synthesized and similarly used in the binding competition assay. M 1 competed for the binding as effectively as the wild-type OL 2, whereas M 2 and M 4 only partially competed, and M 3 failed to compete at all. These results indicate that both B1 and B2 complexes were formed by the binding of proteins through a central sequence, 5′-GGAAGT, defined by mutant M 3, and a couple of the adjacent residues defined by mutants M 2 and M 4. To elucidate the protein-binding residues in more detail, we then used one-point (OP) mutated oligonucleotides spanning both sides of the central sequence in the binding competition

assay (OP 1 to 10 [Fig. 4B]). Among the 5′ OPs (OP 1 to 5), OP 1 and OP 2 competed for the binding as effectively as the wild-type oligonucleotide, whereas OP 3 and OP 4 only partially competed. These results imply that the 5′ edge of the protein-binding sequence is the adenine located at position −505, as defined by OP 3. Surprisingly, OP 5 appeared to have stronger binding affinity for DNA, since it competed more effectively than the wild-type oligonucleotide (Fig. 4B). In the direct binding assay, OP 5 indeed displayed enhanced complex formation (not shown). Since all 3′ OPs (OP 8 to 10) showed the same competition profile as that of the wild-type oligonucleotide (Fig. 4B), the 3′ ends of the central sequence were further mutated (OP 6 and OP 7). Of the two oligonucleotides prepared, OP 6 could not compete for the binding, whereas OP 7 did to some extent. These results indicate that the thymine located at position −497, mutated in OP 7, is the 3′ terminus of the binding sequence and that the guanine, located at position −498, substituted in OP 6, is essential for protein binding. It is important to note that B1 and B2 exhibited identical competition profiles with respect to the mutated oligonucleotides M 2 to 4 and OP 3 to 7 (Fig. 4). On the basis of these results, the sequence requirement and the binding specificity of NF-P1 and NF-P2 are most likely identical (residues −505 through −497, mutated in OP 3 to 5 and M 3). We shall refer to this purine-rich 9-mer sequence, 5′-ACAGGAAGT (−505 to −497), hereafter as the NF-P motif. Subsequent sequence comparison revealed the location of the human cognate NF-P motif, 5′-gCAGGAAGT, being between residues −618 and −610 of human *Pfp* (21).

Positive regulatory function of the NF-P motif. To examine whether the 9-mer sequence identified above is responsible for the positive regulatory function originally observed for the $pCAT_{-566}$ reporter construct, a synthetic oligonucleotide containing in tandem three copies of the residues −522 through −491 sequence was linked 5′ to the *Pfp* sequence in the $pCAT_{-411}$ construct. This construct (designated $pCAT_{oligo}$) was transfected into CTLL-R8 and non-CTL EL-4 cells, and the CAT enzyme activity was monitored in the transfected cell lysates. In several repeating experiments, increased CAT expression over that driven by $pCAT_{-411}$ was found in CTLL-R8 but not in EL-4 cells (Fig. 5A and B). Interestingly, an intermediate level of enhancement of CAT expression occurred when the $pCAT_{oligo}$ was transfected into CTLL-R8 cultured in medium without IL-2 [CTLL-R8 (NC) (Fig. 5B)]. These results suggest that the observed positive regulatory activity is killer cell specific, IL-2 inducible, and likely mediated by the NF-P motif, as no other protein-binding sequence has been identified within this region. Since $pCAT_{-566}$ appeared to be more efficient than $pCAT_{oligo}$ in enhancing the CAT expression, the possibility that additional positive regulatory elements are present within the region of residues −412 through −566 still cannot be ruled out.

To verify further the role of the NF-P motif in the transcription of *Pfp*, two reporter constructs containing the *Pfp* sequence spanning from residue +62 to residue −522 with the NF-P motif being mutated [5′-CACGGAAGT-3′ ($pCAT_{M21}$) and 5′-ACATTCCTG-3′ ($pCAT_{M31}$); mutated as underlined] were prepared. Analyses with the lysates of CTLL-R8 transfected with these constructs showed little or virtually no expression of the CAT gene (Fig. 5C). These results suggest that the integrity of the NF-P motif not only is important for enhancing *Pfp* expression but also is essential for the normal function of downstream regulatory sequences. It appears also that the 5′ sequence flanking the GGAA/T core is critical for the enhancer activity of the NF-P motif.

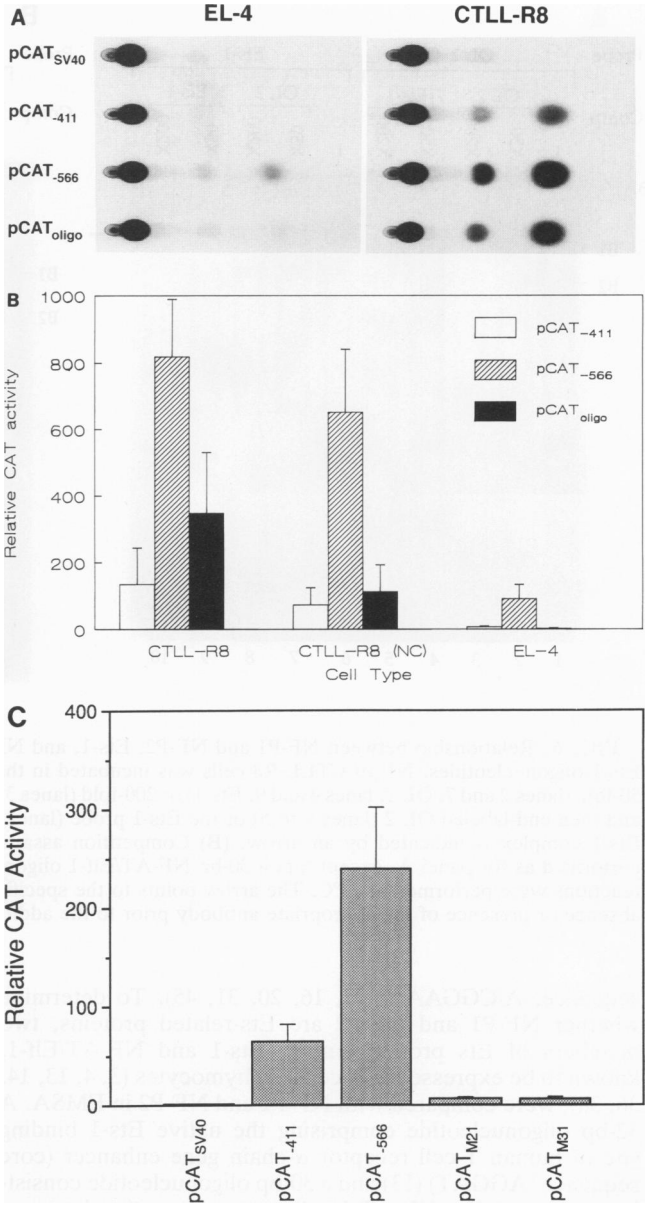

FIG. 5. Functional analysis of the NF-P motif. (A) CTLL-R8 and EL-4 cells were transfected with either of the three reporter constructs: $pCAT_{-411}$, $pCAT_{oligo}$, and $pCAT_{-566}$ (see text). CAT activity in cell lysate was analyzed by thin-layer chromatography. The results shown were derived from a representative experiment. (B and C) CAT activity in the cells transfected with the appropriate construct was measured by liquid scintillation counting. The activities were normalized on the basis of the transfection efficiency and compared with the background expression driven by the control plasmid vector. The data shown represent the mean values derived from three independent experiments. $pCAT_{M21}$ and $pCAT_{M31}$ contain mutations at residues −505 to −503 and −502 to −497, respectively (see text).

Relationship of NF-P1 and NF-P2 with Ets proteins. On the basis of sequence comparison, the purine-rich NF-P motif appeared to be reminiscent of the binding site for the protein products of the *ets* proto-oncogene family (consensus core

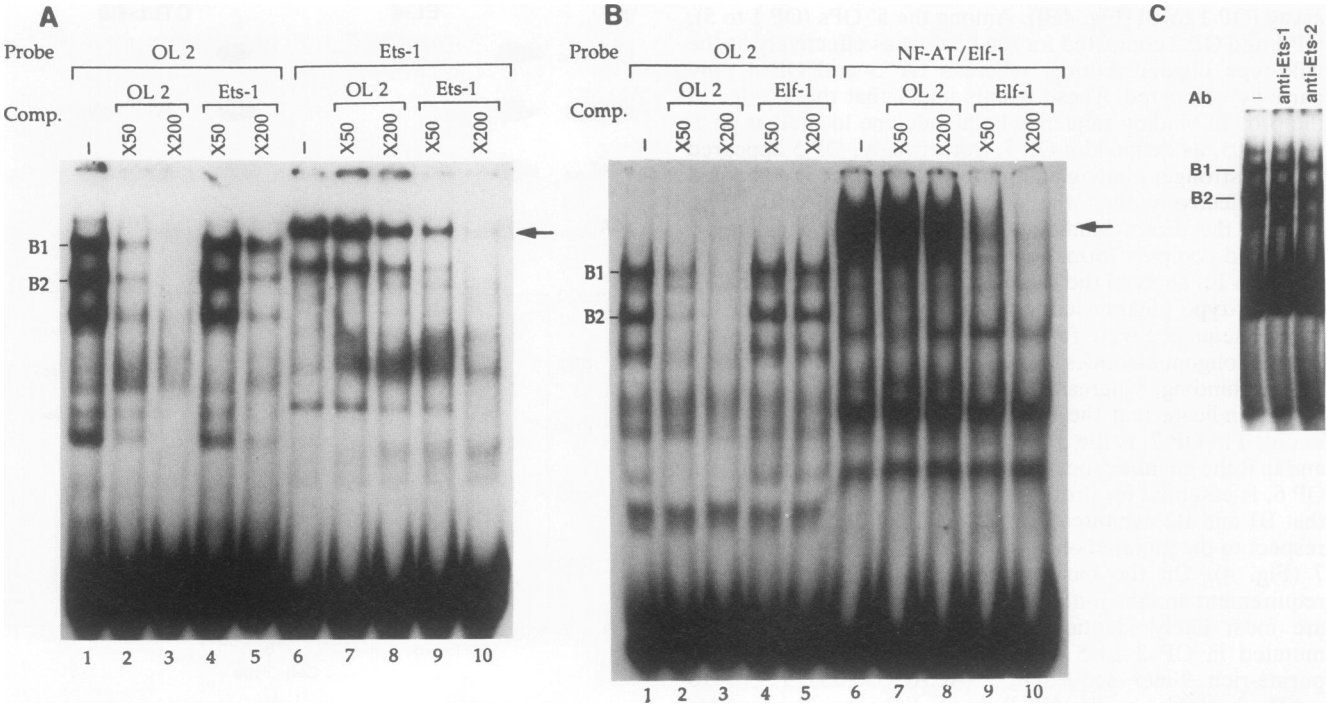

FIG. 6. Relationship between NF-P1 and NF-P2, Ets-1, and NF-AT/Elf-1, analyzed by EMSA. (A) Competition assays with OL 2 and Ets-1 oligonucleotides. NE of CTLL-R8 cells was incubated in the absence of competitor (Comp.) (lanes 1 and 6) or in the presence of a 50-fold (lanes 2 and 7, OL 2; lanes 4 and 9, Ets-1) or 200-fold (lanes 3 and 8, OL 2; lanes 5 and 10, Ets-1) molar excess of unlabeled competitors, and then end-labeled OL 2 (lanes 1 to 5) or the Ets-1 probe (lanes 6 to 10) was added. Both oligonucleotides consist of 32 bp. The specific Ets-1 complex is indicated by an arrow. (B) Competition assays with OL 2 and NF-AT/Elf-1 oligonucleotides. The experiments were performed as for panel A, except that a 30-bp NF-AT/Elf-1 oligonucleotide was used instead of the Ets-1 oligonucleotide, and the binding reactions were performed at 20°C. The arrow points to the specific NF-AT/Elf-1 complex. (C) NE of CTLL-R8 cells was incubated in the absence or presence of the appropriate antibody prior to the addition of end-labeled OL 2 probe.

sequence, A/CGGAA/T) (7, 16, 20, 31, 45). To determine whether NF-P1 and NF-P2 are Ets-related proteins, two members of Ets protein family, Ets-1 and NF-AT/Elf-1, known to be expressed in T cells or thymocytes (3, 4, 13, 14, 36, 38), were compared with NF-P1 and NF-P2 in EMSA. A 32-bp oligonucleotide comprising the native Ets-1 binding site of human T-cell receptor α-chain gene enhancer (core sequence, AGGAT) (13) and a 30-bp oligonucleotide consisting of the native NF-AT binding site (recently shown to interact with Elf-1 and another factor [14, 38]) of the human IL-2 gene enhancer (core sequence, AGGAA, same as the NF-P motif) (12) were used in EMSA, in comparison with the binding of NF-P1 and NF-P2 to OL 2. As shown in Fig. 6, the putative Ets-1 or NF-AT/Elf-1 complex migrated much more slowly than B1 or B2 (Fig. 6A and B, compare lanes 1 and 6), indicating that the molecular masses of NF-P1 and NF-P2 differ significantly from those of the two Ets proteins. To further distinguish NF-P1 and NF-P2 from Ets-1 and Ets-2, EMSA with OL 2 as the probe was performed in the presence of monoclonal antibodies specific for either Ets-1 or Ets-2 (kindly provided by T. S. Papas, National Cancer Institute). These antibodies neither inhibited the formation of B1 and B2 nor shifted the positions of these complexes to a higher-molecular-weight region (the so-called supershift [5]) (Fig. 6C), suggesting that the specific Ets-1 and Ets-2 epitopes recognized by the monoclonal antibodies tested are not present in NF-P1 and NF-P2. In the binding competition analysis, the binding of NF-P1 and NF-P2 to labeled OL 2 was efficiently inhibited by unlabeled OL 2 (Fig. 6A and B, lanes 2 and 3). However, it was only slightly inhibited by the Ets-1 oligonucleotide and not at all inhibited by the NF-AT/Elf-1 oligonucleotide (Fig. 6A and B, lanes 4 and 5). Conversely, unlabeled OL 2 failed to inhibit the formation of the DNA-protein complexes when labeled Ets-1 or NF-AT/Elf-1 probe was used (Fig. 6A and B, lanes 6 to 10). These results strongly suggest that NF-P1 and NF-P2 are distinct from Ets-1 and NF-AT/Elf-1. Nevertheless, the weak cross-competition observed between OL 2 and Ets-1 oligonucleotides (Fig. 6A) implies that NF-P1 and NF-P2 still overlap with Ets-1 to a certain degree in terms of their DNA-binding specificity. Therefore, it is possible that NF-P1 and NF-P2 are also members of the Ets family. They are, however, only distantly related to Ets-1.

Similar-size DNA-binding subunits present in NF-P1 and NF-P2. To estimate the native molecular masses of NF-P1 and NF-P2, NE prepared from resting CTLL-R8 cells was separated on a size-exclusion column, and a portion of each fraction collected was assayed by EMSA for the formation of B1 and B2 complexes. Maximal B1 and B2 formations were detected in fractions 45 and 55, respectively (Fig. 7A). By comparison with molecular mass standards, the native molecular masses of NF-P1 and NF-P2 were estimated to be in the range of 208 to 234 and 91 to 100 kDa, respectively. The DNA-binding specificity of partially purified NF-P1 or NF-P2 was also examined by EMSA with two mutant DNA probes, M 3 and OP 6. The results obtained showed that neither of the two mutant probes formed B1 or B2 complexes with the two factors present in the column fractions (not

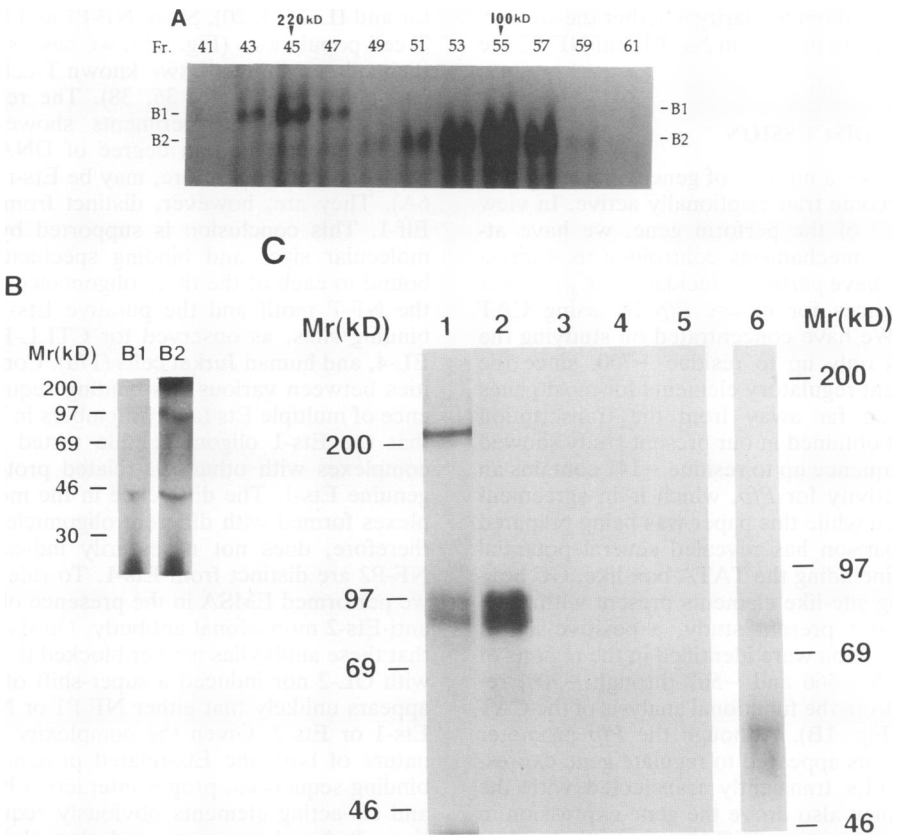

FIG. 7. Molecular masses of NF-P1 and NF-P2. (A) Size-exclusion chromatography. Two milligrams of NE of CTLL-R8 cells was loaded on a Sephacryl S-300 column (50-ml column volume; Pharmacia) that had been equilibrated in 0.1 M KCl–buffer D (18), and 0.5-ml fractions were collected at a flow rate of 0.5 ml/min. Aliquots (20 μl) of each fraction were incubated with labeled OL 2 and then subjected to EMSA. The positions of molecular weight standards eluted are indicated on top of the figure. (B) UV cross-linking analysis of the B1 and B2 complexes. B1 and B2 were resolved by EMSA and subjected to UV irradiation in situ. The cross-linked DNA-protein complexes were electroeluted and analyzed on an SDS–10% polyacrylamide gel under reducing conditions. Left and right lanes, cross-linked B1 and B2 complexes, respectively. (C) UV cross-linking analysis of the B1 and B2 complexes. In situ UV cross-linking was performed with a Stratalinker. The B1 and B2 complexes were eluted by passive diffusion at 4°C and analyzed on an SDS–6% polyacrylamide gel. Lanes 1 and 2, UV-cross-linked B1 and B2, respectively; lane 3, area corresponding to B1 on EMSA performed in the absence of nuclear extract; lanes 4 and 5, un-cross-linked B1 and B2, respectively; lane 6, UV-cross-linked irrelevant DNA-protein complex.

shown). In situ UV cross-linking was then performed to determine the molecular components and the masses of both NF-P1 and NF-P2 under denaturing conditions. In some earlier experiments in which DNA-protein complexes were electroeluted overnight at room temperature, cross-linked B1 and B2 were found to contain several similar-size polypeptide species: two major ones of ~90 and ~40 kDa and, occasionally, a minor one of ~30 kDa (Fig. 7B). Since proteolysis or photocleavage (10) of proteins under harsh experimental conditions was a serious concern, we later adopted a milder UV cross-linking and protein elution protocol. After UV irradiation, the gel slices were incubated at 4°C overnight in soaking buffer containing 1 mM PMSF, during which time DNA-protein complexes would passively diffuse into the buffer. Upon electrophoresis on SDS–6% PAGE (for better resolution of the high-molecular-weight species) under reducing conditions, the ~90-kDa species was resolved into two polypeptide species migrating closely at around 80 to 90 kDa; this was found for both the B1 and B2 complexes (Fig. 7C, lanes 1 and 2). These two 80- to 90-kDa species may represent either two different subunits with similar molecular masses or, instead, isoforms of the same protein. In addition to these dominant doublet bands, two more slowly migrating bands were found in the B1 complex but not in the B2 complex eluate (Fig. 7C, lane 1). Lower-molecular-weight species, probably generated because of incomplete inhibition of proteolysis, were still detected. The cross-linked DNA-protein complexes eluted from an irrelevant third band did not contain the two species migrating at around 80 to 90 kDa (Fig. 7C, lane 6), suggesting that the 80- to 90-kDa doublet species were unique for NF-P1 and NF-P2. These 80- to 90-kDa protein species could not be detected when the nuclear extract was not added during EMSA or if the DNA-protein complexes were not subjected to UV irradiation prior to SDS-PAGE (Fig. 7C, lanes 3 to 5), which indicated that the association between the proteins and oligonucleotides was specific. Taken together, these results suggest that NF-P1 and NF-P2 share a common DNA-binding subunit(s). That NF-P1 and NF-P2 differ in native molecular mass but share similar-size DNA-binding subunits suggests that NF-P1 differs from NF-P2 by having additional non-DNA-binding subunits. It is speculated that the higher-molecular-weight species present in the B1 complex eluate might represent cross-linked entities which contain both the DNA-binding and the non-DNA-binding subunit(s). Additional experiments, in particular the V8

mapping, are being carried out to clarify whether the similar-size DNA-binding subunits present in NF-P1 and NF-P2 are in fact identical.

DISCUSSION

During CTL activation, a number of genes, including that encoding perforin, become transcriptionally active. In view of the tight regulation of the perforin gene, we have attempted to dissect the mechanisms controlling its expression. In this study, we have partially elucidated the promoter and regulatory sequences for mouse *Pfp* by using CAT reporter constructs. We have concentrated on studying the 5′-flanking sequences only up to residue −700, since the promoter and important regulatory elements for most genes usually reside not too far away from the transcription initiation site. Results obtained in our present study showed that the 5′-flanking sequence up to residue −141 contains an essential promoter activity for *Pfp*, which is in agreement with a report published while this paper was being prepared (22). Sequence comparison has revealed several potential regulatory elements, including the TATA box-like, GC box-like, and AP-2 binding site-like elements present within the promoter region. In our present study, a positive and a negative regulatory function were identified in the regions of residues −412 through −566 and −567 through −700, respectively, as judged from the functional analysis of the CAT reporter constructs (Fig. 1B). Although the *Pfp* promoter and the upstream regions appeared to regulate gene expression efficiently in CTLs transiently transfected with the reporter constructs, they also drove the gene expression in non-CTLs in a similar manner. Differing from the results reported by others (22), we have not identified any region that controls *Pfp* expression in a reciprocal fashion in perforin-positive and perforin-negative cells. The reasons for this discrepancy are currently unclear. A more detailed and extensive functional analysis of the 5′-flanking sequences of mouse *Pfp* will be required in order to resolve this issue.

In the present study, we have focused on (i) fine mapping the positive regulatory element present between residues −412 and −566 and (ii) identifying the cognate *trans*-acting factors. By means of EMSA and mutational analysis, we have identified two DNA-binding proteins, NF-P1 and NF-P2, that interact with a particular motif within this region. These two proteins displayed three prominent features. Firstly, NF-P1 was ubiquitously found in all cell types examined, whereas NF-P2 appeared to be present exclusively in killer lymphocytes (Fig. 2A). Secondly, NF-P1 and NF-P2 were reciprocally and specifically modulated in killer cells upon activation (Fig. 2A). Thirdly, both proteins bound to an identical 9-mer purine-rich sequence, 5′-ACAGGA AGT-3′ (residues −505 through −497; designated the NF-P motif [Fig. 4]). All these three features suggest the involvement of NF-P1 and NF-P2 in the cell-type-specific *Pfp* transcription.

Sequence comparison revealed that the NF-P motif is highly homologous to the known binding sites for the Ets proteins, which generally consist of purine-rich 9- to 11-mer sequences with a core motif, GGAA/T (7, 16, 20, 31, 45). The Ets proteins, which are products of the *ets* proto-oncogene family (25, 44), have recently been shown to be a new and large group of transcription activators (16, 25) involved in the transcription of genes encoding a variety of proteins across a wide range of cell types. Several Ets family members have been shown to play a crucial role in the differential expression of T-cell-specific genes, such as the T-cell receptor and IL-2 (13, 20). Since NF-P1 and NF-P2 are present in T-cell populations (Fig. 2A), we have specifically examined their relationship with two known T-cell Ets proteins, Ets-1 and NF-AT/Elf-1 (13, 36, 38). The results obtained from cross-competition experiments showed that NF-P1 and NF-P2 share a certain degree of DNA-binding specificity with Ets-1 and, therefore, may be Ets-related proteins (Fig. 6A). They are, however, distinct from Ets-1 and NF-AT/Elf-1. This conclusion is supported by the differences in molecular sizes and binding specificities of the proteins bound to each of the three oligonucleotide probes encoding the NF-P motif and the putative Ets-1 and NF-AT/Elf-1-binding sites, as observed for CTLL-R8 (Fig. 6), YAC-1, EL-4, and human Jurkat cells (17a). Considering the similarities between various Ets-binding sequences and the presence of multiple Ets family members in T cells, it is possible that the Ets-1 oligonucleotide tested might have formed complexes with other Ets-related proteins, instead of the genuine Ets-1. The difference in the mobilities of the complexes formed with different oligonucleotide probes tested, therefore, does not necessarily indicate that NF-P1 and NF-P2 are distinct from Ets-1. To rule out this possibility, we performed EMSA in the presence of either anti-Ets-1 or anti-Ets-2 monoclonal antibody. On the basis of the results that these antibodies neither blocked the formation of B1-B2 with OL-2 nor induced a super-shift of B1-B2 (Fig. 6C), it appears unlikely that either NF-P1 or NF-P2 is identical to Ets-1 or Ets-2. Given the complexity and the widespread nature of both the Ets-related proteins and their cognate binding sequences, proper interaction between these *trans*- and *cis*-acting elements obviously requires certain regulation. It has been suggested that the differences in the sequences flanking the GGAA/T core play a role in controlling the specific recognition by different Ets family proteins (31, 45). Although an EBS-specific probe, with a sequence highly homologous to the NF-P motif (AgAGGAAGT), could efficiently bind Ets-1 or NF-AT/Elf-1 proteins (43), the genuine NF-P motif exhibited low or virtually no affinity for Ets-1 and NF-AT/Elf-1 (Fig. 6). These results suggest that the 5′ end and/or the flanking nucleotides of the NF-P motif discriminate against various Ets proteins and allow only the specific interaction with NF-P1 and NF-P2. In this respect, it has recently been reported that the 3′-end residues of the EBS may be involved in determining the specific interaction of each EBS motif with its corresponding Ets family member (43). Another possible controlling mechanism is based on the interaction of Ets proteins with other proteins, which then confers the specificity of binding of Ets proteins to unique EBSs (7). Whether this protein-protein interaction also determines the specific binding of NF-P1 and NF-P2 to the NF-P motif still remains to be investigated.

In addition to Ets-1 and NF-AT/Elf-1, three other members of the Ets family, Ets-2, Fli-1, and GABPα, are known to be expressed in T cells (2–4, 19). However, NF-P1 and NF-P2 also seem to be different from all of them. Ets-2 is generally thought to display a binding specificity similar to that of Ets-1 (43, 45) and most likely is distinct from NF-P1 and NF-P2. The inability of anti-Ets-2 antibody to modify the migration of B1-B2 is also in favor of this conclusion. Fli-1 is a single-polypeptide factor (2), whereas NF-P1 and NF-P2 appear to be composed of at least two polypeptide subunits (Fig. 7B and C). GABPα, which forms an $\alpha_2\beta_2$ tetramer with the non-DNA-binding subunit GABPβ (19, 39), possesses a molecular mass of 51 kDa, which is significantly different from those of NF-P1 and NF-P2 (Fig. 7B and C). Furthermore, Fli-1 and GABPα are reported to be

constitutively expressed in thymus and spleen cells (2, 19, 39), while NF-P2 seems to be induced only upon cell activation (Fig. 2A). Although it is unclear whether the expression of Fli-1 and GABPα will be further up-regulated upon cell activation, it is tempting to conclude that, on the basis of the characteristics discussed above, NF-P1 and NF-P2 are distinct from either Fli-1 or GABPα. The definite identities of NF-P1 and NF-P2, nonetheless, can be resolved only when the amino acid or cDNA sequences of these proteins become available.

EBS has been identified in different promoters/enhancers of different viral and mammalian genes. Regulation of the transcription of these genes often correlates with the presence of Ets-related proteins. Most known mammalian Ets family members are expressed in a tissue-specific manner and presumably contribute to the regulation of cell- or tissue-specific gene transcription. For instance, Ets-1 and NF-AT/Elf-1 are preferentially expressed in T cells (3, 36, 38); PU.1 is expressed in macrophage and B cells (17); *elk-1* is expressed in lung and testis (34); and PEA 3 is expressed in epididymis and brain tissue (46). NF-P2 identified in the present study appears to be a novel killer cell-specific Ets-related protein. Although the biological function of this factor remains somewhat obscure, two lines of evidence support the role of NF-P2 as a killer cell-specific activator for mouse *Pfp*. Firstly, NF-P2 was detected only in lymphocytes with a killer phenotype, and its expression could be modulated by reagents known to activate T cells and up-regulate perforin message levels. Secondly, the NF-P motif to which NF-P2 binds was capable of enhancing gene expression when the particular reporter construct ($pCAT_{oligo}$) was transiently expressed in CTLL-R8 but not in EL-4 (Fig. 5). That the functional activity of $pCAT_{oligo}$ did not lead to a greater CAT expression driven by $pCAT_{-566}$ (Fig. 5) implies that the NF-P motif is not the only positive regulatory element present within that region of *Pfp*. In this regard, sequences homologous to the AP-1- and AP-2-binding sites were also identified near the NF-P motif in the 5′-flanking region of mouse *Pfp*. Precedents showing that Ets proteins interact with AP-1 and/or other transcription factors so as to become functionally active have been reported (9, 26, 28, 33). It is likely that, for *Pfp*, NF-P1 and NF-P2 also play a regulatory role by cooperating with proteins bound to either the other regulatory elements or the basal promoter, thereby suppressing or initiating the gene expression in perforin-negative or perforin-positive cells. Since NF-P1 was found to be present in all cell types examined, it may simply bind to the NF-P motif and hence prevent the subsequent binding or interaction of other factors which, together with NF-P2, would form an active transcription machinery. Upon activation of the killer cells, NF-P1 may either be displaced or replaced by NF-P2 or, alternatively, be transformed into NF-P2 (Fig. 8; see below), which then assembles into the effective transcription machinery. Nevertheless, the possibility that NF-P1 could directly suppress the basal and inducible transcription of *Pfp* in non-CTLs and resting CTLs, much like what ETs-1 does to the T-cell receptor-β gene (25), still cannot be ruled out. The precise functions of NF-P1 and NF-P2, therefore, await clarification through further in vitro transcription assays with the purified proteins. The possibility of the NF-P motif as a killer cell-specific regulatory element for *Pfp* is further strengthened by sequence comparison with human *Pfp*. The NF-P motif and its flanking region are found to be also well conserved in the human gene. The sequence between residues −634 and −604 of human *Pfp* is highly homologous to

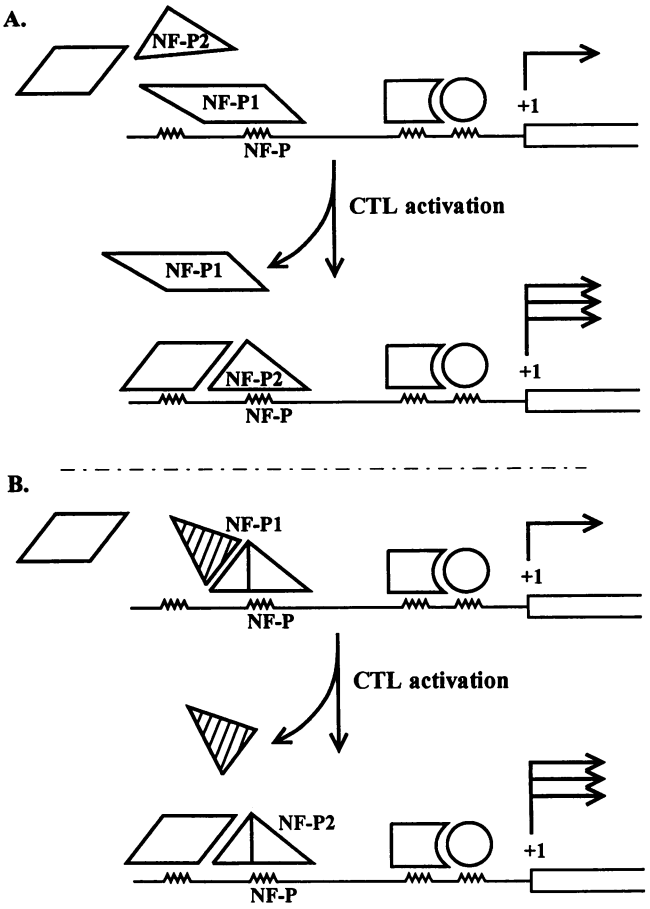

FIG. 8. Hypothetical models for the involvement of the NF-P motif and NF-P1 and NF-P2 in cell-specific transcription of mouse *Pfp*. (A) Upon activation, NF-P1, which originally occupies the NF-P motif and prevents other transcription factors from binding to the nearby regulatory elements, may be expelled. NF-P2 and other factors are now allowed to access the DNA and initiate efficient transcription in a cooperative fashion. (B) The non-DNA-binding subunits which block the binding of other transcription factors are released from the NF-P1 complex upon activation. The trimmed NF-P2 interacts with the other transcription factor and enhances transcription. ○, □, △, and ▱, putative transcription factors; ⁓, putative *cis*-acting regulatory elements; +1, transcription initiation site; ⌐→, gene transcription.

the mouse sequence between residues −522 and −491 (with a 27 of 32 bases identity). Sequence comparison showed that the human NF-P motif counterpart resides between residues −618 and −610, consisting of 5′-gCAGGAAGT (with an eight of nine bases identify to the mouse NF-P). On the basis of this, it is postulated that the highly conserved NF-P motif should play an important role in the perforin gene expression. Systematic mutational analysis addressing the precise function of this motif and its relationship with other potential regulatory elements in controlling killer cell-specific *Pfp* expression is currently being performed.

With respect to the molecular structure of NF-P1 and NF-P2, UV cross-linking experiments revealed that the two factors contained similar-size DNA-binding subunits (Fig. 7B and C). NF-P1, however, had a higher native molecular mass than NF-P2 (Fig. 7A). This difference in molecular mass may be attributed to an additional NF-P1-specific

protein component(s) that does not bind DNA. The postulated non-DNA-binding subunit(s), however, may be in close proximity to DNA. The results obtained from UV cross-linking experiments revealed that two high-molecular-weight species, in addition to the dominant common subunits, were eluted from B1 (Fig. 7C), suggesting that the different subunits of NF-P1 might have been cross-linked together and migrated as undissociated complexes even in the presence of SDS and reducing agent. This kind of close spatial relationship which leads to cross-linking of the non-DNA-binding unit to DNA has previously been reported for GABP (39). Cross-linking of two proteins, which bind to adjacent DNA-binding sequences, forming an SDS-resistant complex, has been observed for PU.1 and its axillary factor (33). The possibility that NF-P1 is an alternative and inactive form of NF-P2 is further supported by our recent finding that NF-P1 may be converted into NF-P2 upon treatment with denaturing agents such as SDS plus Nonidet P-40 or guanidine hydrochloride (13a). A similar model has recently been proposed for the pancreas-specific transcription factor PTF1, in which the nuclear form PTF1α differs from the cytoplasmic form β by an additional protein component which lacks the DNA-binding activity (37). Therefore, it is possible that cell stimulations result in the release of the additional subunit(s) from NF-P1 exclusively in killer lymphocytes for reasons as yet unclear. The loss of the additional subunit(s) may result in the conversion of NF-P1 (transcriptionally inactive) into NF-P2 (transcriptionally active) (Fig. 8B). This postulation is consistent with the B1-B2 modulation observed in EMSA (Fig. 2A), since the hypothetical conversion should lead to the decrease of NF-P1 and the increase of NF-P2, which were indeed observed. In vitro reconstitution and dissociation analyses are being carried out to further test this hypothesis.

ACKNOWLEDGMENTS

We thank Z. A. Cohn and R. M. Steinman for constant support and for critical reading of the manuscript. We also acknowledge A. Granelli-Piperno for providing the NF-AT/Elf-1 oligonucleotide and nuclear extracts of Jurkat cells and for helpful discussion, and K. Barker and G. Kaplan for reading the manuscript.

This work was supported in part by grants from the National Institutes of Health (CA-47307 to J.D.-E.Y. and RO3-DE10525 to B.S.K.), American Cancer Society (CH425), and American Heart Association, New York City Affiliate. M.F.H. is supported by the National Research Council (CNPq)—Brazil and the Fogarty International Center (NIH). J.D.-E.Y. is a Scholar of the Leukemia Society of America. C.-C.L. is currently supported by an Investigatorship from the American Heart Association, New York City Affiliate, and by a Hirschl Career Scientist Award. B.S.K. is also supported by a fund from The Cancer Research Center, Seoul National University, Seoul, Republic of Korea (KOSEF-SRC-56-CRC-21).

REFERENCES

1. **Abken, H., and B. Reifenrath.** 1992. A procedure to standardize CAT reporter gene assay. Nucleic Acids Res. **20:**3527.
2. **Ben-David, Y., E. B. Giddens, K. Letwin, and A. Bernstein.** 1991. Erythroleukemia induction by Friend murine leukemia virus: insertional activation of a new members of the ets gene family, Fli-1, closely linked to c-ets-1. Genes Dev. **5:**908–918.
3. **Bhat, N. K., R. J. Fisher, S. Fujiwara, R. Ascione, and T. S. Papas.** 1987. Temporal and tissue-specific expression of mouse *ets* genes. Proc. Natl. Acad. Sci. USA **84:**3161–3165.
4. **Bhat, N. K., K. L. Komschlies, S. Fujiwara, R. J. Fisher, B. J. Mathieson, T. A. Gregorio, H. A. Young, J. W. Kasik, K. Ozato, and T. S. Papas.** 1989. Expression of *ets* genes in mouse thymocyte subsets and T cells. J. Immunol. **142:**672–678.
5. **Bhat, N. K., and T. S. Papas.** 1992. Characterization and uses of monoclonal antibody derived against DNA binding domain of the ets family of genes. Hybridoma **11:**277–294.
6. **Bradford, M. M.** 1976. A rapid and sensitive method for the quantitation of microgram quantities of protein utilizing the principle of protein-dye binding. Anal. Biochem. **72:**248–254.
7. **Brown, T. A., and S. L. McKnight.** 1992. Specificities of protein-protein and protein-DNA interaction of GABPα and two newly defined ets-related proteins. Genes Dev. **6:**2502–2512.
8. **Dignam, J. D., R. M. Lebovitz, and R. G. Roeder.** 1983. Accurate transcription initiation by RNA polymerase II in a soluble extract from isolated mammalian nuclei. Nucleic Acids Res. **11:**1475–1489.
9. **Dudek, H., R. V. Tantravahi, V. N. Rao, E. S. Reddy, and E. P. Reddy.** 1992. Myb and Ets proteins cooperate in transcriptional activation of the mim-1 promoter. Proc. Natl. Acad. Sci. USA **89:**1291–1295.
10. **Gibbons, I. R., A. Lee-Eiford, G. Mocz, C. A. Phillipson, W.-J. Tang, and B. H. Giobbons.** 1987. Photosensitized cleavage of dynein heavy chains. Cleavage at the "V1 site" by irradiation at 365 nm in the presence of ATP and vanadate. J. Biol. Chem. **262:**2780–2786.
11. **Gorski, K., M. Carneiro, and U. Schibler.** 1986. Tissue-specific *in vitro* transcription from the mouse albumin promoter. Cell **47:**767–776.
12. **Granelli-Piperno, A., and P. McHugh.** 1991. Characterization of a protein that regulates the DNA-binding activity of NF-AT, the nuclear factor of activated T cells. Proc. Natl. Acad. Sci. USA **88:**11431–11434.
13. **Ho, I.-C., N.-H. Bhat, L. R. Gottschalk, T. Lindsten, C. B. Thompson, T. S. Papas, and J. M. Leiden.** 1990. Sequence-specific binding of human Ets-1 to the T cell receptor alpha gene enhancer. Science **250:**814–818.

13a. **Horta, M. F., et al.** Unpublished data.

14. **Jain, J., P. G. McCaffrey, V. E. Valge-Archer, and A. Rao.** 1992. Nuclear factor of activated T cells contains Fos and Jun. Nature (London) **356:**801–804.
15. **Joag, S. V., C.-C. Liu, B. S. Kwon, W. R. Clark, and J. D.-E. Young.** 1990. Expression of mRNAs for pore-forming proteins and two serine esterases in murine primary and cloned effector lymphocytes. J. Cell. Biochem. **43:**81–88.
16. **Karim, F. D., L. D. Urness, C. S. Thummel, M. J. Klemsz, S. R. McKercher, A. Celada, V. Beveren, R. A. Maki, C. V. Gunther, J. A. Nye, and B. J. Graves.** 1990. The ETS-domain: a new DNA-binding motif that recognize a purine-rich core DNA sequence. Genes Dev. **4:**1451–1453.
17. **Klemsz, M. J., S. R. McKercher, A. Celada, C. V. Beveren, and R. A. Maki.** 1990. The macrophage and B cell-specific transcription factor PU.1 is related to the ets oncogene. Cell **61:**113–124.

17a. **Koizumi, H.** Unpublished data.

18. **Koizumi, H., C.-C. Liu, L. M. Zheng, S. V. Joag, N. K. Bayne, J. Holoshitz, and J. D.-E. Young.** 1991. Expression of perforin and serine esterases by human gamma/delta T-cells. J. Exp. Med. **173:**499–502.
19. **LaMarco, K., C. C. Thompson, B. P. Byers, E. M. Walton, and S. L. McKnight.** 1991. Identification of Ets- and Notch-related subunits in GA binding protein. Science **253:**789–792.
20. **Leiden, J. M.** 1992. Transcriptional regulation during T-cell development: the alpha TCR gene as a molecular model. Immunol. Today **13:**22–30.
21. **Lichtenheld, M. G., and E. R. Podack.** 1989. Structure of the human perforin gene. A simple gene organization with interesting potential regulatory sequences. J. Immunol. **143:**4267–4274.
22. **Lichtenheld, M. G., and E. R. Podack.** 1992. Structure and function of the murine perforin promoter and upstream region: reciprocal gene activation or silencing in perforin positive and negative cells. J. Immunol. **149:**2619–2626.
23. **Liu, C.-C., S. V. Joag, B. S. Kwon, and J. D.-E. Young.** 1990. Induction of perforin and serine esterases in a murine cytotoxic T lymphocyte clone. J. Immunol. **144:**1196–1201.
24. **Liu, C.-C., S. Rafii, A. Granelli-Piperno, J. A. Trapani, and J. D.-E. Young.** 1989. Perforin and serine esterase gene expression in stimulated human T cells: kinetics, mitogen require-

ments, and effect of cyclosporin A. J. Exp. Med. **170:**2105–2118.
25. **Macleod, K., D. Leprince, and D. Stehelin.** 1992. The ets gene family. Trends Biochem. Sci. **17:**251–256.
26. **Majerus, M. A., F. Bibollet-Ruche, J. B. Telliez, B. Wasylyk, and B. Bailleul.** 1992. Serum, AP-1 and Ets-1 stimulate the human ets-1 promoter. Nucleic Acids Res. **20:**2699–2703.
27. **Maniatis, T., S. Goodbourn, and J. A. Fischer.** 1987. Regulation of inducible and tissue-specific gene expression. Science **236:** 1237–1244.
28. **Mavrothalassitis, G. J., and T. S. Papas.** 1991. Positive and negative factors regulate the transcription of the ETS2 gene via an oncogene-responsive-like unit within the ETS2 promoter region. Cell Growth Diff. **2:**215–224.
29. **Mitchell, P. J., and R. Tjian.** 1989. Transcriptional regulation in mammalian cells by sequence-specific DNA binding proteins. Science **245:**371–378.
30. **Molitor, J. A., W. H. Walker, S. Doerre, D. W. Ballard, and W. C. Greene.** 1990. NF-κB: a family of inducible and differentially expressed enhancer-binding proteins in human T cells. Proc. Natl. Acad. Sci. USA **87:**10028–10032.
31. **Nye, J. A., J. M. Pertersin, C. V. Gunther, M. D. Jonsen, and B. J. Graves.** 1992. Interaction of murine Ets-1 with GGA-binding sites establishes the ETS domain as a new DNA-binding motif. Genes Dev. **6:**975–990.
32. **Podack, E. R., H. Hegartner, and M. G. Lichtenheld.** 1991. A central role of perforin in cytolysis? Annu. Rev. Immunol. **9:**129–157.
33. **Pongubala, J. M. R., S. Nagulapalli, M. J. Klemsz, S. R. McKercher, R. A. Maki, and M. L. Atchison.** 1992. PU.1 recruits a second nuclear factor to a site important for immunoglobulin κ 3′ enhancer activity. Mol. Cell. Biol. **12:**368–378.
34. **Rao, V. N., K. Huebner, M. Isobe, A. Ar-Rushdi, C. M. Croce, and E. P. S. Reddy.** 1989. *elk*, tissue-specific *ets*-related genes on chromosomes X and 14 near translocation breakpoints. Science **244:**66–70.
35. **Scheidereit, C., J. A. Cromlish, T. Gerster, K. Kawakami, C.-G. Balmaceda, R. A. Currie, and R. G. Roeder.** 1988. A human lymphoid-specific transcription factor that activates immunoglobulin genes is a homeobox protein. Nature (London) **336:** 551–557.
36. **Shaw, J.-P., P. J. Utz, D. B. Durand, J. J. Toole, E. A. Emmel, and G. R. Crabtree.** 1988. Identification of putative regulator of early T cell activation genes. Science **241:**202–205.
37. **Sommer, L., O. Hagenbuchle, P. K. Wellauer, and M. Strubin.** 1991. Nuclear targeting of the transcription factor PTF1 is mediated by a protein subunit that does not bind to the PTF1 cognate sequence. Cell **67:**987–994.
38. **Thompson, C. B., C.-Y. Wang, I.-C. Ho, P. R. Bohjanen, B. Petryniak, C. H. June, S. Miesfeldt, L. Zhang, G. J. Nabel, B. Karpinski, and J. M. Leiden.** 1992. *cis*-acting sequence required for inducible interleukin-2 enhancer function bind a novel Ets-related protein, Elf-1. Mol. Cell. Biol. **12:**1043–1053.
39. **Thompson, C. C., T. A. Brown, and S. L. McKnight.** 1991. Convergence of ets- and notch-related structural motifs in a heteromeric DNA-binding complex. Science **153:**762–768.
40. **Trapani, J. A., and B. Dupont.** 1990. Novel putative promoter/enhancer sequences are shared by the mouse and human perforin gene. Tissue Antigens **36:**228–234.
41. **Trapani, J. A., B. S. Kwon, C. A. Kozak, C. Chintamaneni, J. D.-E. Young, and B. Dupont.** 1990. Genomic organization of the pore-forming protein (perforin) gene and localization to chromosome 10: similarities to and differences from C9. J. Exp. Med. **171:**545–557.
42. **Tschopp, J., and M. Nabholz.** 1990. Perforin-mediated target cell lysis by cytolytic T lymphocytes. Annu. Rev. Immunol. **8:**279–302.
43. **Wang, C.-Y., B. Petryniak, I.-C. Ho, C. B. Thompson, and J. M. Leiden.** 1992. Evolutionarily conserved Ets family members display distinct DNA binding specificities. J. Exp. Med. **175:** 1391–1399.
44. **Watson, D. K., R. Ascione, and T. S. Papas.** 1990. Molecular analysis of the Ets genes and their products. Crit. Rev. Oncog. **1:**409–436.
45. **Woods, D. B., J. Ghysdael, and M. J. Owen.** 1992. Identification of nucleotide preferences in DNA sequences recognised specifically by c-Ets-1 protein. Nucleic Acids Res. **4:**699–704.
46. **Xin, J.-H., A. Cowie, P. Lachance, and J. A. Hassell.** 1992. Molecular cloning and characterization of PEA3, a new member of the Ets oncogene family that is differentially expressed in mouse embryonic cells. Genes Dev. **6:**481–496.
47. **Youn, B.-S., C.-C. Liu, K.-K. Kim, J. D.-E. Young, M. H. Kwon, and B. S. Kwon.** 1991. Structure of the mouse pore-forming protein (perforin) gene: analysis of transcription initiation site, 5′ flanking sequence, and alternative splicing of 5′ untranslated regions. J. Exp. Med. **173:**813–822.
48. **Young, J. D.-E.** 1989. Killing of target cells by lymphocytes: a mechanistic view. Physiol. Rev. **69:**250–314.
49. **Zychlinsky, A., M. Karim, R. Nonacs, and J. D.-E. Young.** 1990. A homogeneous population of lymphokine-activated killer (LAK) cells is incapable of killing virus-, bacteria-, or parasite-infected macrophages. Cell. Immunol. **125:**261–267.